



# Tumor feeding artery reconstruction with multislice spiral CT in the diagnosis of pelvic tumors of unknown origin

Hai-Jing Hu\*, Yong-Wen Huang\*, Ying-Chang Zhu

## PURPOSE

We aimed to compare multislice spiral computed tomography (MSCT) angiography diagnosis with both surgical findings and postoperative pathological results in patients with pelvic tumors of unknown origin. In addition, the diagnostic accuracy of MSCT angiography was compared with that of routine computed tomography for tumor feeding artery volume reconstruction to determine the origin and nature of pelvic tumors.

## MATERIALS AND METHODS

The records of 43 patients with pelvic tumors of unknown origin who underwent MSCT angiography were retrospectively reviewed. Volume reconstructions using add vessel and merge views methods were performed for abdominal and pelvic blood vessels. The tumor origin was identified based on observations of the origin, number, morphology, starting/ending locations, route, and distribution of the tumor feeding arteries.

## RESULTS

Overall, the mean tumor diameter was  $9.8 \pm 3.5$  cm (range, 4.2–23.5 cm); 11 tumors (25.6%) were cystic in nature; and 32 tumors (74.4%) were either solid/cystic or solid in nature. When considering all MSCT angiography examinations used to predict the nature of the tumor (e.g., malignant or benign), the sensitivity and specificity were 77.3% and 95.2%, respectively. The positive and negative predictive values were 94.4% and 80%, respectively. The overall diagnostic accuracy was 86.05% with an area under the curve of 0.961 (95% confidence interval, 0.913–1.000).

## CONCLUSIONS

MSCT angiography volume reconstruction for pelvic tumor feeding arteries of unknown origin is highly valuable for localization, qualitative diagnosis, and quantitative diagnosis of pelvic tumors.

Primary pelvic tumors of unknown origin often have an insidious onset and atypical symptoms. Conventional computed tomography (CT) diagnosis relies on the anatomical position and spatial relationship between adjacent organs. Therefore, this modality has a low (55%) diagnostic accuracy (1–3). In contrast, multislice spiral CT (MSCT) angiography is a noninvasive and comprehensive method for evaluating pelvic tumors of unknown origin, and use of this method could improve visualization of the small blood vessels as well as the quality of vascular imaging in such tumors (4). MSCT angiography reconstructs tumor feeding arteries using the add vessel (AV) method; and provides visualization of the three-dimensional spatial relationship between the tumor, tumor feeding arteries, and adjacent organs and large blood vessels using the merge views (MV) method. This ensures both an accurate and reliable display of the pelvic tumor feeding arteries.

In recent years, the application of multislice spiral CT has improved the rate of diagnostic accuracy in pelvic tumors (5). MSCT angiography is mainly used to evaluate the blood vessels of clearly diagnosed abdominopelvic tumors prior to surgery (6). However, few reports exist describing the use of MSCT AV and MV volume reconstruction to determine pelvic tumor feeding artery origins, identify benign or malignant tumors, and differentiate between primary or secondary tumors. Some individuals recommend using magnetic resonance angiography for imaging pelvic tumor feeding arteries (7), even as MSCT angiography is emerging as the diagnostic tool of choice.

In fact, an increasing number of studies have demonstrated the importance of diagnostic imaging for determining the nature of pelvic tumors. MSCT angiography has an emerging clinical role in vascular imaging. It has potentially significant advantages over conventional angiography and CT scans in pelvic tumor diagnosis, especially with regard to differentiating between benign and malignant disease states and assisting in disease management (8–12).

The purpose of this study was to compare diagnoses made using MSCT angiography with both surgical findings and postoperative pathological results in patients with pelvic tumors of unknown origin. In addition, the diagnostic accuracy of MSCT angiography was compared with that of routine CT for tumor feeding artery volume reconstruction to determine the origin and nature of pelvic tumors.

## Materials and methods

### Subjects

In this retrospective study, the records of patients diagnosed with pelvic tumors of unknown origin who received precontrast, arterial phase,

From the Departments of Radiology (H.H.) and Surgery (Y.Z. ✉ zhuyingchang@163.com), Nanhai Hospital, Nanfang Medical University, Foshan, Guangdong, China; the Department of Gynecology (Y.H.), State Key Laboratory of Oncology in South China, Sun Yat-sen University Cancer Center, Guangzhou, Guangdong, China.

\*Hai-Jing Hu and Yong-Wen Huang contributed equally to this work.

Received 28 December 2012; revision requested 24 January 2013; revision received 20 May 2013; accepted 6 June 2013.

Published online 8 October 2013.  
DOI 10.5152/dir.2013.12176

and venous phase imaging between May 2007 and November 2010 were reviewed. Inclusion criteria included preliminary diagnosis of pelvic tumors of unknown origin and postop/postbiopsy diagnostic confirmation of the pelvic tumors. This study was approved by the Institutional Review Board of Nanhai Hospital, and the requirement of patient informed consent was waived due to the retrospective study design.

#### *Imaging protocol and postprocessing*

A 64-row multidetector spiral CT scanner (GE LightSpeed Ultra multidetector spiral CT scanner, GE Medical Systems, Milwaukee, Wisconsin, USA) was used. Each patient received a single CT scan, in which they underwent precontrast, arterial phase, and venous phase imaging. The range of the scan was from the top of the diaphragm to the pubic symphysis. The scan parameters were 120 kV, 160–180 mAs, with a slice thickness of 5 mm, slice interval of 5 mm, reconstructed section thickness of 1.25 mm, and a reconstruction interval of 0.625 mm. Individuals were injected with 90–100 mL of the non-ionic contrast agent iopamidol 300 mg L/mL (Iopamiro, Bracco S.P.A., Milano, Italy) at an injection rate between 3.5–4.0 mL/s. The scan delay times in the arterial and venous phases were 25–32 s and 60–90 s, respectively. Tumor staining was indicated by both tumor neovascularization and the concentration of the contrast agent in the tumor vasculature. The median radiation dose (plain+contrast-enhanced scan) was 1586 mGy.cm (range, 1386.87–1986.21 mGy.cm). The radiation dose was in accordance with internationally accepted CT dosage regimens.

Initially, multiplanar reconstruction was used in combination with the original enhanced axial images to preliminarily determine both pelvic tumor position and morphology. Simultaneously, AV and MV volume reconstruction were utilized for postprocessing of images (Advantage Window 4.3 Work Station, Sun Microsystems, Mountain View, California, USA). The original enhanced images were used to locate the cross-section of the tumor feeding arteries in the source image; this was recognized as the imaging threshold.

The AV method was used to generate blood vessels with the same threshold; these were tracked using the density of the source blood vessels. The following vascular volume reconstruction images were reconstructed: tumor feeding arteries and their branches, the collateral feeding artery, and the abdominal aorta with its branches. The display parameters (window width, window level, transparency, brightness, and color) for the three reconstructed images were adjusted. Finally, MV volume reconstruction was used for the image display to accurately describe the anatomical relationship between the tumor feeding arteries, surrounding blood vessels, and the tumor itself.

#### *Image analysis*

Two senior radiologists specializing in CT angiography were blinded to the pathology reports and independently interpreted the routine MSCT angiography images. If a discrepancy arose, they arrived at a consensus after joint review of the images. The following types of pelvic tumors of unknown origin were included in the study: primary nonpelvic origin tumors, small pelvic origin tumors, and exogenous or ectopic pelvic tumors. The criteria for differentiating between benign and malignant tumors using CT images obtained in a standard CT protocol (plain+contrast-enhanced) were based on standard definitions (13).

#### *Tumor staining and the route of feeding arteries and newly formed vessels*

Tumor staining refers to both neovascularization in and around the tumor, as well as the concentration of contrast agent in the tumor vasculature. It is represented by the increased mean three-dimensional pixel value within the tumor (i.e., CT value in Hounsfield Units [HU]) after MSCT angiography when compared with the CT value of the same area in routine CT images (i.e., plain+contrast-enhanced CT). The attenuation value was evaluated in reformatted images relative to the arterial phase. Arterial phase data were used to calculate tumor staining. The tumor staining classification is presented in Supplemental Table 1.

The feeding artery and newly formed vessel routes were classified by vessel distributions. A regular route was defined as a tumor feeding artery travelling along the tumor edge, clearly outlining the tumor contour with uniform intratumoral vascular distribution and a clearly displayed tumor profile. An irregular route was defined as a tumor feeding artery that did not completely outline the tumor contour, with uneven intratumoral vascular distribution and only partially displayed tumor profile.

The origin, number, morphology, starting/ending locations, route, and distribution of the tumor feeding artery were observed after abdominopelvic blood vessel reconstruction. The diagnostic criteria based on the tumor feeding artery included a thickened feeding artery with a trunk or branch entering the tumor and a mesh-like or radial vessel distribution, morphologically distributed around the tumor edge (Supplemental Table 2) (14).

#### *Statistical analysis*

Patient age and tumor diameters were summarized using mean±standard deviation or median with (range, minimum–maximum) if the data were not normally distributed. The tumor, resection types, origin, and tumor feeding artery characteristics displayed by MSCT angiography were given as numbers (n) for a given specific tumor type. The MSCT angiography examination measurements between postoperative pathology-based diagnosis (i.e., benign and malignant in nature) were compared using a Mann-Whitney U test due to the ordinal or non-normally distributed data. Univariate and multivariate logistic regression analysis was performed to evaluate the diagnostic accuracy of MSCT angiography. The receiver operating characteristic curve with respective area under the curve (AUC) at a 95% confidence interval (CI) was calculated, as were the accuracy rate, sensitivity, specificity, positive predictive value (PPV), and negative predictive value (NPV). The diagnostic accuracy of routine CT scans was summarized as n (%), by the nature of CT examination. All statistical assessments were considered two-tailed, and the

**Table 1.** Demographic and clinical data, and origin of tumor feeding arteries with respect to tumor type determined by MSCT angiography (n=43)

Variables	Tumor type							Total
	Primary ovarian tumor	Metastatic ovarian tumor	Exogenous uterine tumor	Colon tumor	Neurogenic tumors	Embryoblastic tumor	Lymphoma	
n	23	3	3	6	4	3	1	43
Age (years)	60.7±9.0 (39–76)	69 (68–75)	57 (51–60)	66 (43–73)	51 (45–69)	29 (19–53)	58 (NA)	58.8±11.9 (19–76)
Tumor diameter (cm)	9.1±3.0 (4.2–18.0)	16.8 (11.0–23.5)	9.2 (8.3–12.3)	8.3 (6.3–13.2)	9.6 (6.6–10.2)	9.7 (7.9–12.1)	9.8 (NA)	9.8±3.5 (4.2–23.5)
Tumor characteristics								
Cystic	8	0	0	0	0	3	0	11
Solid and cystic or solid	15	3	3	6	4	0	1	32
Resection type								
Surgical resection	21	0	3	5	4	3	1	37
Biopsy	2	3	0	1	0	0	0	6
Origin of tumor feeding arteries determined by MSCT angiography								
Unilateral ovarian branch of the uterine artery	15	1	0	0	0	0	0	16
Unilateral ovarian artery	11	0	0	0	0	0	0	11
Ovarian branches of bilateral uterine arteries	5	2	3	0	0	0	0	10
Superior and inferior mesenteric arteries	0	0	0	6	0	0	0	6
Median and lateral sacral artery	0	0	0	0	4	0	0	4
Other branches of the abdominal aorta	3	0	0	0	0	0	0	3
Superior and inferior gluteal artery	0	0	0	0	0	3	0	3
Bilateral ovarian arteries	2	0	0	0	0	0	0	2
Unnamed branch of the internal iliac artery	0	0	0	0	0	0	1	1

MSCT, multislice spiral computed tomography; NA, not applicable.

Patients' age and tumor diameters are presented as the mean±standard deviation for primary ovarian tumor group and median (range, minimum–maximum) for other groups (except lymphoma group) due to the insufficient number of patients; tumor characteristics, resection type, and origin of tumor feeding arteries, as determined by MSCT angiography, are presented as the frequency for each group.

level of significance was set at  $P < 0.05$ . The data were analyzed using a commercially available software (Statistical Package for Social Sciences, version 18.0, SPSS Inc., Chicago, Illinois, USA).

## Results

A total of 43 patients, 35 females and eight males, with a mean age of 58.8±11.9 years (range, 19–76 years) were included in the analysis. Tumor specimens were obtained from 37 subjects (86%) by surgical resection and from six subjects (14%) by biopsy. Patient demographics, tumor characteristics and MSCT angiography reconstruction (feeding artery origin by

tumor type) are displayed in Table 1. Overall, the mean tumor diameter was 9.8±3.5 cm (range, 4.2–23.5 cm). Eleven subjects (25.6%) had cystic tumors and 32 subjects (74.4%) had either solid/cystic tumors or solid tumors. MSCT angiography examination measurements compared with postoperative pathological diagnosis are shown in Table 2. Significant differences in MSCT angiography measurements were noted between benign and malignant lesions ( $P < 0.05$  for all).

Diagnostic results of MSCT angiography for tumor characteristics are summarized in Table 3. MSCT angiography demonstrated an accuracy ranging

from 83.7% to 88.4% for determining whether a tumor was benign or malignant. The method of differentiating benign and malignant tumors based on the number of main feeding artery branches had a sensitivity of 77.3%, specificity of 90.5%, PPV of 89.5%, and NPV of 79.2%. Differentiation based on the route of feeding arteries and newly formed vessels had a sensitivity of 68.2%, specificity of 100%, PPV of 100%, and NPV of 75%. Differentiation based on the distribution of newly formed vessels had a sensitivity of 81.8%, specificity of 90.5%, PPV of 90%, and NPV of 82.6%. Differentiation based on tumor staining

**Table 2.** Comparison of MSCT angiography measurements by postoperative pathological diagnosis (n=43)

Characteristics of feeding arteries (MSCT angiography)	Postoperative pathological diagnosis		<i>P</i> <sup>a</sup>
	Malignant	Benign	
n	22	21	
Number of main feeding artery branches			< 0.001
1	5 (22.7)	19 (90.5)	
2	10 (45.5)	2 (9.5)	
3	5 (22.7)	0	
4	2 (9.1)	0	
Pattern associated with both route and newly formed vessels of the feeding artery			< 0.001
Irregular	15 (68.2)	0	
Regular	7 (31.8)	21 (100)	
Distribution of newly formed blood vessels	49.45 (11.50–70.00)	11.50 (6.40–24.10)	< 0.001
Tumor staining	45.25 (7.80–61.30)	7.80 (3.40–10.00)	< 0.001
None	5 (22.7)	21 (100)	< 0.001
Weakly positive	2 (9.1)	0	
Positive	4 (18.2)	0	
Strongly positive	11 (50)	0	

<sup>a</sup>*P* < 0.05 indicates a significant difference between benign and malignant tumors. *P* values were derived using the Fishers' exact test with Yate's correction for categorical variables or the Mann-Whitney U test for non-normal continuous variables and ordinal continuous variables.

MSCT, multislice spiral computed tomography.

The data are presented as n (%) for categorical variables and ordinal continuous variables; or median (range, minimum–maximum) for continuous variables lacking normal distribution.

tative diagnosis of pelvic tumors of unknown origin was significantly below that of MSCT angiography.

## Discussion

Our results showed that MSCT angiography has both a high specificity and high positive predictive value in addition to a remarkable rate of diagnostic accuracy as reflected by the high AUC value. This finding was similar to those of other studies such as Catalano et al. (14), in which MSCT angiography delivered excellent results in assessing abdominopelvic tumor vascular involvement. Pelvic tumors of unknown origin often have an occult onset with atypical symptoms; common bladder, prostatic, or gynecologic causes should be ruled out during the initial assessment (8). Imaging is required to distinguish between gynecological, gastrointestinal, and neurogenic origin tumors as all can present similarly in the pelvic region (1). However, radiologists often have difficulties in diagnosis of exogenous and ectopic tumor origins using routine CT, as a wide spectrum of benign and malignant pathology present similarly in terms of shape, structure, enhancement, origin, and localization (10). Hence, diagnostic accuracy of pelvic tumors of unknown origin is traditionally low (1, 2). Due to anatomical restriction by the pelvis, large tumors can occupy the entire pelvis or extend into the abdominal cavity, leading to exogenous growth. Therefore, MSCT angiography has advantages as both a useful ancillary diagnostic procedure and as an imaging method in complex cases (4, 11, 12, 14). MSCT angiography can also assess arteriovenous vascularization in patients with different abdominal pathologies and evaluate exogenous and ectopic abdominopelvic tumors of unknown origin (14). MSCT angiography can also identify tumor feeding vessels to aid in surgical planning, allowing for optimal management by the appropriate medical team (14, 15).

Catalano et al. (14) found that MSCT angiography can be quite helpful in diagnosing source organs or tissues for abdominopelvic tumors of unknown origin by providing visualization of the origin, number, morphology, starting and ending locations, route, and

had a sensitivity of 77.3%, specificity of 100%, PPV of 100%, and NPV of 80.8%. Combining all MSCT angiography measurements resulted in a sensitivity of 77.3%, specificity of 95.2%, PPV of 94.4%, and NPV of 80% for distinguishing benign from malignant lesions. The diagnostic accuracy rate was 86.05% when all MSCT angiography measurements were considered, with an AUC value of 0.961 (95% CI, 0.913–1.000).

One patient had preoperatively diagnosed synchronous tumors confirmed by postoperative pathology. The tumors included a left-side teratoma and right ovary cystadenoma, which were supplied by the left uterine artery ovarian branch and right ovarian feeding arteries, respectively (Fig. 1). This case of synchronous pelvic tumors was diagnosed preoperatively based on both MSCT angiography and original CT images. One patient had a metastatic pelvic tumor and a single metastatic lesion in the anterior rectal wall, exterior to the primary ovarian tumor. In

this case, the collateral blood supply was supplied by both the innominate branch of the right internal iliac artery and the rectal artery (Fig. 2). The branches of the rectal artery at the second level showed a filling defect caused by a tumor thrombus. The tumor metastases to the pelvis and the rectum were diagnosed based on both MSCT angiography and original CT images, and these results were confirmed by postoperative pathological examination.

Routine CT results demonstrated a localization accuracy for pelvic tumors of unknown origin of 55.8%, an accuracy of qualitative tumor diagnosis (i.e., malignant vs. benign) of 58.2%, and an accuracy of quantitative tumor diagnosis (i.e., single vs. multiple tumors) of 83.7%. A comparison of the diagnostic accuracy to determine benign vs. malignant lesions using routine CT and MSCT angiography is shown in Supplemental Table 3. The accuracy of routine CT for the localization, qualitative diagnosis and quanti-

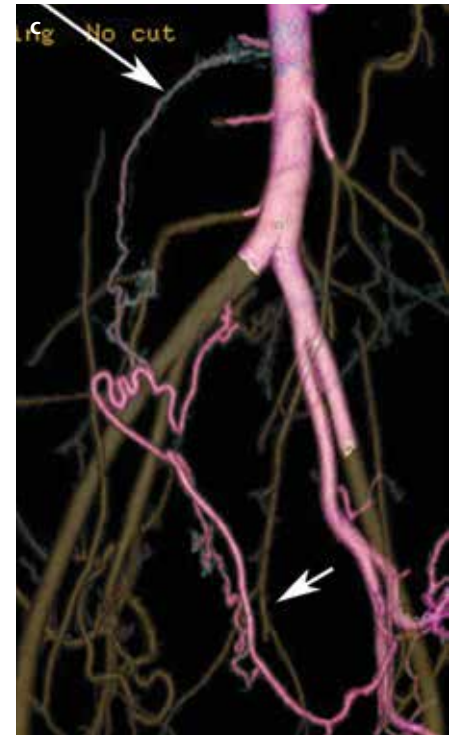


**Figure 1. a–c.** Bilateral ovarian tumors with multiple origins consisting of a right ovarian cystadenoma and a left ovarian teratoma. The sagittal image of the enhanced CT (a) shows both solid septal and cystic masses (arrow); the axial image of the enhanced CT (b) shows both lipid and calcification components in the solid area (CT values: short arrow, -80 HU; long arrow, 670 HU); MSCT angiography volume reconstruction image (c) shows that the tumors had different origins and the feeding arteries originated from different locations. The teratoma was fed by the ovarian branch of the left uterine artery (short arrow), and the ovarian cystadenoma was fed by the right ovarian artery (long arrow). The tumor feeding artery was single, and the route was regular. No neovascularization or tumor staining was present.

distribution of the tumor feeding arteries. Similarly, a study by Zhang et al. (16) showed that the tumor feeding artery leads directly to the tumor's origin. Other studies by Liu et al. (17) and White et al. (18) traced the origin of ovarian and uterine tumors from ovarian or uterine arteries, respectively. These studies found that uterine tumor feeding arteries typically arose from the internal iliac artery, while ovarian tumor feeding arteries were direct branches of the abdominal aorta (17, 18). Our study supports these results, documenting that the feeding arteries of pelvic-origin tumors originated either from branches of the abdominal aorta or the internal iliac artery. Feeding arteries of nonpelvic organ tumors originated from the abdominal wall branches of either the abdominal aorta or internal iliac artery. Neoplasms of pelvic origin, such as ovarian tumors, often show exogenous growth due to the small size of the source organ. A small number of these tumors form ectopic masses directly in the abdominopelvic cavity. In such cases, the source organ is often disfigured, and thus, it can be difficult to differentiate such tumors from tumors arising from abdominal organs (1, 8–10). Imaging can reveal characteristics that differentiate the origin of pelvic tumor, es-

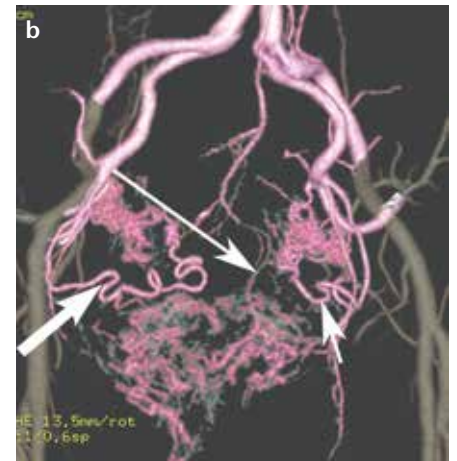
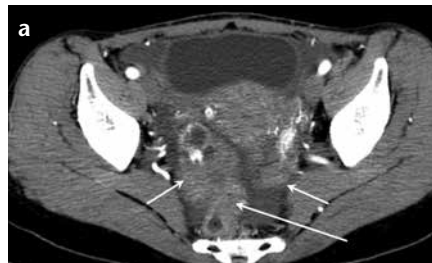


**Figure 2. a, b.** Multiple pelvic tumors representing bilateral ovarian papillary serous cystadenocarcinomas and metastatic rectal carcinomas. The axial image of the enhanced CT (a) shows bilateral ovarian multiple solid tumors (short arrows) and anterior rectal wall hypertrophy (long arrow); MSCT angiography volume reconstruction image (b) shows that the tumor had three main feeding arteries: the ovarian branches of the bilateral uterine arteries (short arrow) and the rectal branch of the inferior mesenteric artery (long arrow). The feeding artery branches show a tortuous and irregular route. The newly formed blood vessels were dense and showed positive tumor staining (thick arrow).

pecially gynecological origin tumors from non-gynecological origin tumors (1). Our study used MSCT angiography to reconstruct the feeding arteries and found that the ovarian tumor blood supply shared many characteristics with the normal physiological ovarian blood supply. A majority of the feeding arteries were ovarian branches of the uterine artery; a small portion of the feeding arteries were from the ovarian artery. There were 23 primary ovarian tumors in this study. In 20 of

the cases, the feeding arteries originated from the ovarian branch of the uterine artery and/or the ovarian artery; all cases were clearly diagnosed before surgery. In the remaining three cases, the feeding arteries were derived from the branches of the abdominal aorta (e.g., the superior mesenteric artery and renal artery); these arteries were misdiagnosed as supplying intestinal and renal tumors prior to surgery. Kronenke et al. (19) found that the ovarian artery could also be anomalously

**Table 3.** Diagnostic results of MSCT angiography in comparison to postoperative pathological results (n=43)

Model #	Predictors	Predicted status		Accuracy %	Sensitivity %	Specificity %	PPV %	NPV %	AUC	95% CI
		Malignant	Benign							
1	Number of branches of the main feeding artery	19	24	83.72	77.30	90.50	89.50	79.20	0.854	0.734–0.974
2	Pattern of travel and newly formed blood vessels of the feeding artery	15	28	83.72	68.20	100	100	75	0.841	0.714–0.967
3	Distribution of newly formed blood vessels	20	23	86.05	81.80	90.50	90	82.60	0.938	0.870–1.000
4	Tumor staining	17	26	88.37	77.30	100	100	80.80	0.922	0.843–1.000
5	1+2	21	22	88.37	86.40	90.50	90.50	86.40	0.917	0.824–1.000
6	1+3	19	24	88.37	81.80	95.20	94.70	83.30	0.961	0.911–1.000
7	1+4	20	23	86.05	81.80	90.50	90	82.60	0.952	0.895–1.000
8	2+3	20	23	86.05	81.80	90.50	90	82.60	0.938	0.870–1.000
9	2+4	17	26	88.37	77.30	100	100	80.80	0.922	0.843–1.000
10	3+4	17	26	88.37	77.30	100	100	80.80	0.937	0.869–1.000
11	1+2+3	19	24	88.37	81.80	95.20	94.70	83.30	0.961	0.911–1.000
12	1+2+4	20	23	86.05	81.80	90.50	90	82.60	0.952	0.895–1.000
13	1+3+4	18	25	86.05	77.30	95.20	94.40	80.00	0.961	0.913–1.000
14	2+3+4	17	26	88.37	77.30	100	100	80.80	0.937	0.869–1.000
15	1+2+3+4	18	25	86.05	77.30	95.20	94.40	80	0.961	0.913–1.000

AUC, area under the receiver operating characteristic curve; CI, confidence interval; MSCT, multislice spiral computed tomography; NPV, negative predictive value; PPV, positive predictive value.

The results were derived using both univariate and multivariate logistic regression model analysis. Models 5–15 were constructed using various combinations of predictors in models 1–4 as shown in the Table above.

derived pairwise from either the anterior circumference of the abdominal aorta below the renal hilum or the accessory renal artery. Hence, variable origins of the ovarian tumor feeding artery may present difficulties in determining the origin of abdominopelvic tumors (17–19), as was the case for several patients in our study.

Our study also demonstrated the capability to determine ovarian tumor blood supply origin. This was possible if the MSCT angiography blood vessel reconstruction demonstrated that the main tumor feeding artery was either the ovarian branch of the uterine artery and/or the ovarian artery. This variation in blood supply was similar to findings from previous studies by Liu et al. (17) and White et al. (18), in which pelvic tumors received supply from both the ovarian and uterine arteries. In some cases in our study, it was difficult to locate variable feeding artery origins of ovarian tumors on standard CT; hence, MSCT angiography

was useful for differentiation. For example, the ovarian branch of the uterine artery supplying ovarian tumors is thinner than the branch of the uterine artery that normally supplies leiomyomas. The uterine artery branches have high MSCT angiography enhancement rates, while the ovarian branches of the uterine arteries do not enhance on MSCT angiography. Scans of leiomyomas only showed visualization of the uterine artery branch, whereas imaging of ovarian tumors often demonstrates visualization of both ovarian and uterine artery branches (17, 18). Our study also found that in exogenous uterine tumors, the main tumor feeding arteries were branches of the uterine artery trunk. The feeding arteries and bilateral uterine arteries traveled towards the uterus and entered the tumor at the junction between the uterus and the tumor. Hence, there were overlapping vascular supply regions, resulting in blood supply anastomoses similar to previous findings of Liu et al. (17)

and White et al. (18). Further evaluation determined that this tumor was exogenous and most likely originated from the uterus. Sun et al. (3) also reported that neoplasms with intestinal origin, such as gastrointestinal stromal tumors or exogenous colorectal cancer, present with similar findings to exogenous uterine tumors. These neoplasms often originate from the intestinal wall, with conventional CT images showing intratumoral gas shadows and main feeding arteries originating from mesenteric artery branches of the corresponding intestinal segments (2, 3). In our study, the colonic tumors were fed by the superior and inferior mesenteric artery branches, consistent with previous reports. Likewise, Brocker et al. (20) and Kinkel et al. (21) found CT scanning to be a useful instrument for evaluating pelvic tumors.

The results of our study suggest that most pelvic tumors of unknown origin (36/43, 83.72%) are fed by abdominal aorta and internal iliac artery branches.

Nonorgan primary tumors were rare and were mainly distributed in the anatomical rectal pouch and space (22). In our study, four cases of neurogenic tumors and three cases of gestational trophoblastic tumors were found in the perirectal and retrorectal spaces, respectively. The most common feeding arteries for pelvic tumors were the wall branches of the abdominal aorta and internal iliac artery, the median sacral artery, the lateral sacral artery, and the superior and inferior gluteal arteries, consistent with results from the earlier report (22). The single case of lymphoma in our study was comprised of a tumor with poor blood supply. Therefore, this tumor could not be accurately located before surgery.

Studies have shown that the benign or malignant nature of tumors is related to the route, number, and morphology of the tumor parenchymal feeding arteries. The presentation of tumor feeding arteries is useful in differentiating between benign and malignant tumors (14). Most of cystic tumors in our study were benign with a single feeding artery that traveled upward along the tumor edge and terminated at the periphery of the cyst wall. Additionally, the feeding artery had no mesh-like branches within the tumor, consistent with the findings of Zhang et al. (16). Mixed cystic and solid pelvic tumors and solid pelvic tumors can be either benign or malignant (7–9). In our study, malignant tumors usually had two or more feeding arteries of different origins, while benign tumors were mainly fed by a single blood vessel. Only a few (2/21, 9.52%) benign tumors were fed by two feeding arteries, in which the tumor feeding artery travelled into the parenchyma and entered the lesion. The feeding arteries of benign tumors demonstrated regular routes with fewer branches, while malignant tumors were fed by multiple arteries that displayed more disorderly and uneven mesh-like branches. Benign tumor feeding arteries were accompanied by neovascularization, tumor staining, and associated tumor vasculature. In our study, MSCT angiography had an 86% accuracy rate for differentiation between benign and malignant tumors. Therefore, we believe that MSCT angiography recon-

struction of tumor blood vessels has a definite value in differentiating between benign and malignant pelvic tumors of unknown origin. Preoperative MSCT angiography can be beneficial in evaluating both tumoral and adjacent tissue vascular structure, which may reduce postoperative complications (14, 15, 23).

When multiple abdominopelvic tumors are present, it is difficult to use conventional CT imaging to determine whether the tumors are from single or multiple origins (16). The results of our study showed that the main feeding artery origin differs depending on tumor origin. Multiple nonfused pelvic parenchymal tumors can arise from different origins; this diagnosis may occur if the feeding arteries supplying the tumor parenchymal areas derive from different sides, or if there is no overlap between different vascular trunks and their supplied areas (17, 18). However, when multiple implanted foci and metastases of the same tumor type are present, the metastatic tumor feeding artery can also arise from many origins and provide multiple blood supplies to the corresponding non-fused tumor parenchyma (17, 18). Therefore, it is difficult to differentiate metastatic lesions and tumors from multiple origins based only on tumor feeding artery characteristics. It is generally believed that tumor feeding arteries often overlap with metastatic feeding arteries in abdominopelvic tumors (16). A more accurate judgment can be made if CT imaging displays consistent tumor distribution, density, morphology, and enhancement, and if the feeding artery has a symmetrical distribution. Our study showed that when the tumor invaded the surrounding tissues and organs, the feeding artery of the invaded organ was dilated and its branches were tortuous and dilated. Large amounts of tumor emboli observed in both the affected organ feeding artery and tumor parenchymal artery branches created vascular blockage, leading to uneven vessel density. This finding allows CT images to differentiate between tumors of metastatic origin and those originating from multiple organs (16). However, if only a small amount of tumor foci invade the surrounding tissue and organ, those metastatic foci

cannot be detected on conventional CT images. The feeding artery of the affected organ is very thin, and even MSCT angiography cannot reconstruct the tumor feeding artery. Therefore, misdiagnoses or missed diagnoses may easily occur. Nevertheless, studies such as Huang et al. (24) and our current study have demonstrated that MSCT angiography can accurately provide information to differentiate between abdominopelvic organ arteries, veins and tumor supply vessels.

There were several limitations associated with this study. First, due to the lower socioeconomic status of the majority of the Chinese population, additional digital subtraction angiography could not be performed. Imaging studies for most patients were not compared with digital subtraction angiography images, i.e., the gold standard. Hence, a true analysis could not be made based on established methods. In addition, some of diagnostic criteria in this study overlapped between benign and malignant tumors. For example, challenges exist in determining the distribution of newly formed vessels (sparse in both benign and malignant tumors) as well as tumor staining; the route of the established and newly formed vessels may overlap (17, 18). Therefore, MSCT angiography cannot achieve a 100% diagnostic accuracy rate. To resolve this issue, the final diagnosis should include conventional CT images to achieve a higher accuracy in determining tumor nature. Finally, as the key operating technique in this study relies on the feeding artery display, associations between the amount of the solid tumor composition, richness of the tumor blood supply, and filling of contrast agent in the tumor feeding artery should also be considered.

In conclusion, reconstructing feeding arteries in pelvic tumors of unknown origin using AV and MV volume reconstruction may improve the accuracy of location, qualitative diagnosis, and quantitative diagnosis for such tumors. This is accomplished through revealing the origin, number, morphology, distribution, and route of the feeding arteries. Through these findings, MSCT angiography provides detailed information for selecting optimal clinical treatment protocols.

## Supplemental tables

Supplemental tables of this manuscript are available online at <http://dx.doi.org/10.5152/dir.2013.12176>

## Conflict of interest disclosure

The authors declared no conflicts of interest.

## References

1. Foshager MC, Hood LL, Walsh JW. Masses simulating gynecologic disease at CT and MR imaging. *Radiographics* 1996; 16:1085–1099.
2. Yoshitake T, Asayama Y, Yoshimitsu K, et al. Bilateral ovarian leiomyomas CT and MRI features. *Abdom Imaging* 2005; 30:117–119. [\[CrossRef\]](#)
3. Sun CH, Li ZP, Meng JF, Xu DS. Value of CT and endoscopic ultrasound in the diagnosis of gastrointestinal stromal tumors. *Zhonghua Fang She Xue Za Zhi* 2004; 38:197–201.
4. Iannaccone R, Laghi A, Passariello R. Multislice CT angiography of mesenteric vessel. *Abdom Imaging* 2004; 29:146–152. [\[CrossRef\]](#)
5. Oto A, BaĖgün N, Kutluk T, Eryilmaz M, Oran M, Besim A. Intraperitoneal involvement in in rhabdomyosarcoma CT findings in a child. *Turk J Pediatr* 2001; 43:342–344.
6. Horton KM, Fishman EK. Multidetector CT angiography of pancreatic carcinoma: part I, evaluation of arterial involvement. *Am J Radiol* 2002; 178:827–831.
7. Balan P. Ultrasonography computed tomography and magnetic resonance imaging in the assessment of pelvic pathology. *Eur J Radiol* 2006; 58:147–155. [\[CrossRef\]](#)
8. Vahidi K, Joe BN, Meng M, Coakley FV, Yeh BM. Review of atypical pelvic masses on CT and MRI; expanding the differential diagnosis. *Clin Imaging* 2007; 31:406–413. [\[CrossRef\]](#)
9. Chang WC, Meux MD, Yeh BM, et al. CT and MRI of adnexal masses in patients with primary nonovarian malignancy. *Am J Radiol* 2006; 186:1039–1045.
10. Padovan RS, Karalik M, Prutki M, Hrabak M, Oberman B, Potocki K. Cross-sectional imaging of the pelvic tumors and tumor-like lesions in gynecologic patients—misinterpretation points and differential diagnosis. *Clin Imaging* 2008; 32:2296–2302. [\[CrossRef\]](#)
11. Wintersperger BJ, Nikolau K, Becker CR. Multidetector-row CT angiography of the aorta and visceral arteries. *Semin Ultrasound CT MR* 2004; 25:25–40. [\[CrossRef\]](#)
12. Smith CL, Horton KM, Fishman EK. Mesenteric CT angiography: a discussion of techniques and selected applications. *Tech Vasc Intervent Rad* 2006; 9:150–155. [\[CrossRef\]](#)
13. Ros PR, Morteale, KJ. CT and MRI of the abdomen and pelvis: a teaching file. 2nd ed. Lippincott Williams & Wilkins, 2007; 399–480.
14. Catalano C, Laghi A, Fraioli F, et al. High-resolution CT angiography of the abdomen. *Abdom Imaging* 2002; 27:479–487. [\[CrossRef\]](#)
15. Zeleniuk BI, Adamian LV, Obel'chak IS, Khoroshun ND. Role of multislice spiral computed tomographic angiography in the treatment of uterine myoma. *Vestn Rentgenol Radiol* 2012; 3:34–37.
16. Zhang YH, Jin CZ, Tan WC, Lin XH, Zhang YZ, Xu XC. Value of MSCTA in the diagnosis of the origin of the ectopic abdominal ovarian tumors. *Zhonghua Fang She Xue Za Zhi* 2009; 43:365–368.
17. Liu FY, Wang MQ, Duan F, Wang ZJ, Song P. Ovarian artery supply is one of the factors affecting the interventional therapeutic efficacy of pelvic tumors. *Zhonghua Zhong Liu Za Zhi* 2009; 31:62–65.
18. White AM, Banovac F, Yousefi S, Slack RS, Spies JB. Uterine fibroid embolization: the utility of aortography in detecting ovarian artery collateral supply. *Radiology* 2007; 244:291–298. [\[CrossRef\]](#)
19. Kroencke TJ, Kawamoto S, Fishman EK. Ovarian artery variant: another unexpected extrarenal condition that may affect donor nephrectomy. *Radiographics* 2004; 24:1513–1514. [\[CrossRef\]](#)
20. Bocker KA, Alt CD, Eichbaum M, Sohn C, Kauczor HU, Hallscheidt P. Imaging of female pelvic malignancies regarding MRI, CT, and PET/CT: part 1. *Strahlenther Onkol* 2011; 187:611–618. [\[CrossRef\]](#)
21. Kinkel K, Lu Y, Mehdizade A, Pelte MF, Hricak H. Indeterminate ovarian mass at US: incremental value of second imaging test for characterization—meta-analysis and Bayesian analysis. *Radiology* 2005; 236:85–94. [\[CrossRef\]](#)
22. Goss PE, Schwertfeger L, Blackstein ME, et al. Extragonadal germ cell tumors. A 14-year Toronto experience. *Cancer* 1994; 73:1971–1979. [\[CrossRef\]](#)
23. Xie E, Weng ZS, Wang XZ, Huang YK. Clinical significance of multi-slice spiral CT angiography in radical resection of gastric cancer. *Zhonghua Wei Chang Wai Ke Za Zhi* 2011; 14:31–33.
24. Huang JH, Fan WJ, Li CJ, et al. Application of multislice spiral CT angiography on transcatheter arterial chemoembolization for hepatocellular carcinoma. *Ai Zheng* 2009; 28:159–163.

**Supplemental Table 1.** Definitions of tumor staining categories

Tumor staining	Definition
None	Increase in CT value was $\leq 10$ HU in the contrast agent-concentrated area of the tumor after enhancement when compared to the CT value of the same area on routine CT (i.e., plain + contrast-enhanced CT). The tumor contour could not be distinguished.
Weakly positive	Increase in CT value was $> 10$ HU but $\leq 30$ HU, and the tumor contour was partially observed.
Positive	Increase in CT value was $> 30$ HU but $\leq 50$ HU, and the tumor contour was clearly outlined.
Strongly positive	Increase in CT value was $> 50$ HU, and the tumor contour could be fully visualized as the contrast agent was highly concentrated.

CT, computed tomography; HU, Hounsfield Unit.

**Supplemental Table 2.** Differential diagnosis of benign and malignant tumors based on the tumor feeding artery and original image characteristics

Nature of tumor	Characteristics of feeding arteries seen in MSCT angiography			Tumor staining	Characteristics of the tumor cyst wall (original image)
	Number of main feeding artery branches	Distribution of newly formed blood vessels	Route of the feeding artery and newly formed blood vessels		
Benign	1 or 2	None or sparse	Regular	No	The tumor cyst wall was evenly thickened without enhancement
Malignant	$\geq 2$	Sparse or dense	Irregular	Positive or strongly positive	The local tumor cyst wall was unevenly thickened with enhancement

MSCT, multislice spiral computed tomography.

**Supplemental Table 3.** Comparison of the diagnostic accuracy between routine CT and MSCT angiography

	Diagnosed n (%)	Undiagnosed n (%)	<i>P</i> <sup>a</sup>
Routine CT examination	25 (58.19)	18 (41.81)	-
Diagnostic accuracy of MSCT angiography examination			
Model #1	36 (83.7)	7 (16.3)	0.020
Model #2	36 (83.7)	7 (16.3)	0.020
Model #3	37 (86.0)	6 (14.0)	0.014
Model #4	38 (88.4)	5 (11.6)	0.010
Model #5	38 (88.4)	5 (11.6)	0.010
Model #6	38 (88.4)	5 (11.6)	0.010
Model #7	37 (86.0)	6 (14.0)	0.014
Model #8	37 (86.0)	6 (14.0)	0.014
Model #9	38 (88.4)	5 (11.6)	0.010
Model #10	38 (88.4)	5 (11.6)	0.010
Model #11	38 (88.4)	5 (11.6)	0.010
Model #12	37 (86.0)	6 (14.0)	0.014
Model #13	37 (86.0)	6 (14.0)	0.014
Model #14	38 (88.4)	5 (11.6)	0.010
Model #15	37 (86.0)	6 (14.0)	0.014

<sup>a</sup>*P* values were derived using the McNemar test to identify differences between diagnostic results of MSCT angiography examination and routine CT examination.

MSCT, multislice spiral computed tomography.

Models are described in Table 3.